

ELECTROWEAK BARYOGENESIS AT AND AFTER PREHEATING: WHAT'S THE DIFFERENCE? *

Dmitri Grigoriev [†]

*Institute for Nuclear Research of Russian Academy of Sciences,
60th October Anniversary Prospect, 7a, Moscow 117312, Russia*

Two recent scenarios of preheating-related baryogenesis are compared within the framework of Abelian Higgs model in (1+1) dimensions. It is shown that they shift baryon number in opposite directions. Once both scenarios can realize simultaneously as overlapped stages of the same physical process, even the sign of net generated asymmetry becomes dependent on initial parameters.

*To appear in the Proceedings of XXXVth Rencontres de Moriond: Electroweak Interactions and Unified Theories, Les Arcs, France, 11-18 March 2000.

[†]e-mail: dgr@inr.ac.ru

As it was shown recently, parametric resonance during preheating opens new possibilities for electroweak baryogenesis [1, 2] which can take place both during [3] and after [4] the resonance. While baryogenesis mechanisms described in [3] and [4] can appear in the same theory and even overlap in the course of the same parametric resonance, they are based on different dynamic effects. In the present paper we compare baryoproducing efficiency of both mechanisms and discuss underlying dynamical processes. The key difference between these mechanisms is that they are related to different time scales existing in the model. Baryogenesis at preheating exists on rather short parametric resonance time scale, while baryogenesis after preheating is related to inflaton thermalization time scale, that can become very large, at least in classical dynamics [6]. The third time scale is the Higgs field thermalization time which generally lies between the two previous time scales. This intermediate time scale defines the freeze-out time of post-resonant sphaleron transitions and is important because sphaleron transitions may wash out the generated asymmetry if they'll keep going after the end of baryoproduction. While the wash-out processes as well as other fermion backreaction effects are beyond the scope of our numerical simulations, the very existence of intensive sphaleron transitions on the time scale considerably larger than baryoproduction time is a signal for possible problems.

The resonance-localized baryogenesis [3] can rapidly produce considerable shift in topological number. Unlike baryogenesis at first-order phase transition, it occurs during extended period of time on the resonance time scale, thus making the wash-out problem a bit easier to solve. However, in this case wash-out suppression requires rather short Higgs thermalization time which should be close to resonance time scale. An attempt to achieve this in (1+1)-dimensional theory being simulated in [3] leads to unacceptably high reheating temperatures $T_{\text{rh}} \sim 0.3 v$ where sphaleron transitions do not freeze out at all, see Fig. 8 of [3]. Even though this conjecture isn't directly applicable to realistic (3+1)-dimensional case, it shows that more efficient ways to prevent wash-out are highly desirable.

A promising approach was suggested in paper [4] where it was shown that for certain parameter values baryogenesis keeps going much longer than the resonance itself. In fact, CP violation that drives baryoproduction is present here for very long time, and baryoproduction keeps going as long as the sphaleron transitions occur. This scenario is based on difference between inflaton and Higgs thermalization times. In our simulations Higgs field thermalizes much faster than inflaton field because it couples to gauge field and has nonlinear self-potential, which results in intensive rescattering of Higgs spectral modes. As we will show below, the presence of non-thermalized oscillating inflaton field can generate effective CP violation, which exists on the inflaton thermalization time scale, the longest one in the model. Of course, this CP violation can change the baryon number only via sphaleron transitions, so the baryogenesis actually occurs on Higgs thermalization time scale, freezing out together with the sphaleron transitions. The major advantage of approach [4] is that the baryoproduction-driving effective chemical potential exists here long after the sphaleron transitions vanish. In other words, it gives us a toy model of electroweak baryogenesis which is completely free from wash-out.

An interesting peculiarity of baryogenesis at and after preheating is that both these scenarios can realize simultaneously, see Fig. 2. Once for the same initial parameters they generate baryonic asymmetry of opposite signs, reflecting the fact that underlying dynamical mechanisms are entirely different, the initial conditions determine not only the magnitude, but also the sign of the net shift in baryonic number.

1 Baryogenesis at preheating

Dynamical principles of baryogenesis at preheating are relatively simple (for detailed description of physical framework, Lagrangian and dimensionless units used below see Ref. [3]). Energy transfer from inflaton field into low-momentum modes of Higgs field results in high rate of inequilibrium sphaleron transitions that appear very soon after the beginning of resonance (see Figs. 8 and 14 of paper [3]). On the other hand, in the course of resonance the Higgs v.e.v. $\langle\phi^*\phi\rangle$ comes from zero to its post-resonant value close to 1. Similar to earlier models of baryogenesis at first-order phase transition (see e.g. [5]), the time evolution of Higgs field gives rise to effective chemical potential μ_{eff} that appears through CP-breaking term $-\kappa|\phi|^2\epsilon_{\mu\nu}F^{\mu\nu}$ in Lagrangian. In the presence of sphaleron transitions, this chemical potential drives the Chern-Simons number $N_{\text{CS}} = \frac{1}{2\pi} \int A_1 dx$ in certain direction (see Figs. 11 and 16 of Ref. [3] and Fig. 1 below), thus producing the fermions. In our case, the chemical potential is [3, 4]

$$\mu_{\text{eff}} = -4\pi\kappa\partial_0\langle\phi^*\phi\rangle \quad (1)$$

and has nonzero value only while $\langle\phi^*\phi\rangle$ keeps changing.

The transition of $\langle\phi^*\phi\rangle$ to its stationary value isn't instant (see Fig. 10 of [3]); it takes about the same time as the resonance itself, which is generally much slower than the first-order phase transition. This is an important advantage of baryogenesis at preheating over previous scenarios, because extended baryoproduction time is essential for reducing possible destruction of the created baryons by post-resonant sphaleron transitions, although sphaleron freeze-out is related to Higgs thermalization and occurs on different time scale.

A common way of estimating the baryoproduction in this and similar models is the use of diffusion equation for Chern-Simons number:

$$\frac{dN_{\text{CS}}}{dt} = -\Gamma_{\text{sph}} \frac{\mu_{\text{eff}}}{T_{\text{eff}}} \quad (2)$$

where Γ_{sph} is the rate of sphaleron transitions and T_{eff} — certain effective temperature. Note that Eq. 16 of [3] coincides with Eq. (2) when $\Gamma_B = 0$ (the latter condition reflects the lack of fermionic backreaction in our simulations). Once the $\langle\phi^*\phi\rangle$ value is increasing in the course of resonance, Eqs. (1) and (2) give the sign of ΔN_{CS} :

$$\frac{\Delta N_{\text{CS}}}{\kappa} \propto -\frac{\mu_{\text{eff}}}{\kappa} \propto \partial_0\langle\phi^*\phi\rangle > 0 \quad (3)$$

Eq. (2) can be used for rough estimate of total generated asymmetry by assuming final $\langle\phi^*\phi\rangle$ to be 1:

$$\Delta N_{\text{CS}} \sim \frac{4\pi\kappa}{T_{\text{eff}}} \langle\Gamma_{\text{sph}}\rangle \quad (4)$$

giving $\Delta N_{\text{CS}} \sim -20$ for Fig. 1 and $\Delta N_{\text{CS}} \sim -30$ for Fig. 2. While the first estimate is correct within factor of 2, the latter one has the wrong sign and is off by an order of magnitude. This discrepancy cannot be explained by simplifications used for getting Eqs. (3) and (4).

Indeed, it isn't obvious that the diffusion equation Eq. (2) can be reliably applied to strongly nonequilibrium dynamics of parametric resonance. We check this point directly by substituting $\langle\phi^*(t)\phi(t)\rangle$ and $\Gamma(t)$ measured in numerical simulations [3] into Eqs. (1) and (2), taking $T_{\text{eff}} = T_{\text{rh}}$ and numerically integrating over time, see Figs. 1 and 2. The only source of uncertainty in this check is the effective temperature T_{eff} present in Eq. (2). Exact

physical sense of this quantity isn't completely clear; however, Figs. 6 and 13 of Ref. [3] show that various effective temperatures stay rather close to final equilibrium value T_{rh} and their time variations wouldn't considerably affect the time integral of Eq. (2).

As is clear from Fig. 1, even for high reheating temperatures the Eq. (2) is adequate only for rough qualitative analysis of N_{CS} evolution. It cannot reproduce correctly the short-time dynamics of N_{CS} and provides no explanation for the end of baryoproduction at time ~ 1800 . Both problems are unrelated to possible variations in T_{eff} which are slow and disappear at time ~ 1500 , see Fig. 6 of Ref. [3]. For lower $T_{\text{rh}} \sim 0.09 E_{\text{sph}}$ the diffusion equation (2) is no longer able to give correct sign of final asymmetry, see Fig. 2. It is natural to suppose that the evolution of N_{CS} cannot be reduced to simple diffusion described by Eq. (2) and is sensitive to more subtle dynamical effects. A good example of complicated dynamics beyond the scope of Eq. (2) is the baryogenesis after preheating.

2 Baryogenesis after preheating

The driving force for baryogenesis after preheating [4] is the inflaton field that keeps coherently oscillating after incomplete parametric resonance (see Figs. 2 and 3 of Ref. [4]). Inflaton zero mode decays through thermalization which in our case is very slow. Its oscillations considerably modify Higgs field effective potential

$$V(\phi) = \frac{\lambda}{4}(|\phi|^2 - v^2)^2 + \frac{1}{2}g^2\sigma^2|\phi|^2 \quad (5)$$

thus making inflaton zero mode $\langle\sigma^2\rangle$ and Higgs v.e.v. $\langle\phi^*\phi\rangle$ to oscillate coherently. In its turn, $\langle\phi^*\phi\rangle$ oscillations generate periodic CP-nonconservation through Eq. (1) and also trigger the sphaleron transitions that become synchronized to inflaton/Higgs oscillations. Interplay between these two strongly correlated processes results into steady shift of N_{CS} in direction opposite to that one predicted by diffusion equation (2).

In this section we will analyze dynamics of Chern-Simons number N_{CS} in the presence of oscillating μ_{eff} . Then, taking into account time correlations to Higgs-triggered sphaleron transitions, we show why N_{CS} actually shifts in direction opposite to baryogenesis at preheating.

2.1 CP - $\langle\phi^*\phi\rangle$ correlations

Due to time derivative in μ_{eff} , Eq. (1), periodical oscillations of $\langle\phi^*\phi\rangle$ clearly affect N_{CS} behavior. For $\kappa = 0$, N_{CS} is oscillating uncorrelated to $\langle\phi^*\phi\rangle$ with its own characteristic frequency $\omega_0 = M_W \sim 1$ (these oscillations are averaged out on the plots), while introduction of non-zero κ makes the N_{CS} dynamics dominated by μ_{eff} even for relatively small $\kappa \sim 0.1$, see Fig. 3. The amplitude of N_{CS} oscillations at non-zero κ can be estimated using equation of motion [3, 4] for A_1 field. Let's assume that N_{CS} is oscillating around its steady integer value N_0 which is the topological index of current system vacuum. Making large gauge transformation to vacuum with zero topological index and denoting the new Chern-Simons number as $\delta N_{\text{CS}} = N_{\text{CS}} - N_0$, one gets

$$\delta\ddot{N}_{\text{CS}} + 2\langle\phi^*\phi\rangle\delta N_{\text{CS}} = \frac{L}{2\pi} \cdot 2\kappa\partial_0\langle\phi^*\phi\rangle \quad (6)$$

(we assume the Higgs field to be homogeneous, i.e. neglect all its higher-momentum modes except the zero mode), and

$$\delta N_{\text{CS}} = \frac{i\omega_\sigma}{\omega_0^2 - \omega_\sigma^2} \cdot \frac{\kappa L}{\pi} \delta\langle\phi^*\phi\rangle \quad (7)$$

Here $\delta\langle\phi^*\phi\rangle = Ae^{i\omega_\sigma t}$ (A is the amplitude of $\langle\phi^*\phi\rangle$ oscillations), $\omega_\sigma^2 = 4g^2\langle\phi^*\phi\rangle$ is the frequency of inflaton oscillations, and $\omega_0^2 = 2\langle\phi^*\phi\rangle = M_W^2$ is the proper frequency of free N_{CS} oscillations not visible on Fig. 3. Once $g^2 \ll 1$, we can neglect $\omega_\sigma^2 \ll \omega_0^2$ and further simplify Eq. (6):

$$\delta N_{\text{CS}} = \frac{\kappa L}{2\pi} \frac{\partial_0\langle\phi^*\phi\rangle}{\langle\phi^*\phi\rangle} = -\frac{L}{4\pi^2} \frac{\mu_{\text{eff}}}{\langle\phi^*\phi\rangle} \quad (8)$$

Both eqs. (7) and (8) result in the phase shift between δN_{CS} and $\delta\langle\phi^*\phi\rangle$ being exactly $\frac{\pi}{2} \text{sign } \kappa$. This phase relation actually determines the sign of baryonic asymmetry generated by $\Gamma - CP$ correlations.

2.2 $\Gamma_{\text{sph}} - \langle\phi^*\phi\rangle$ correlations and baryoproduction

Once $\langle\phi^*\phi\rangle$ is oscillating periodically, time averaging of μ_{eff} (1) and δN_{CS} (8) will give zero. In our case this does not mean zero baryoproduction, because the sphaleron transitions occur synchronously to the same oscillations of $\langle\phi^*\phi\rangle$, thus favouring certain values of μ_{eff} .

The correlations between sphaleron transitions and $\langle\phi^*\phi\rangle$ oscillations are discussed in more detail in paper [4]. It is quite natural, however, that most transitions occur at $\langle\phi^*\phi\rangle$ close to its minimum (see Figs. 4 and 6 of Ref. [4]), once this corresponds to minimal E_{sph} . Note that at these moments $\mu_{\text{eff}} \propto \partial_0\langle\phi^*\phi\rangle = 0$, so $\langle\mu_{\text{eff}}\Gamma_{\text{sph}}\rangle = 0$. In other words, Eq. (2) fails even after accounting for correlations between μ_{eff} and Γ_{sph} . Therefore, baryogenesis after preheating involves dynamical effects that are time-nonlocal. Once most topological transitions occur when $\langle\phi^*\phi\rangle$ is at minimum, $\langle\phi^*\phi\rangle$ value is decreasing during the whole half-period of $\langle\phi^*\phi\rangle$ oscillation immediately preceeding the transition, so $\partial_0\langle\phi^*\phi\rangle < 0$ and μ_{eff} has non-zero value of certain sign. According to Eq. (8), $\delta N_{\text{CS}}/\kappa \propto \partial_0\langle\phi^*\phi\rangle < 0$ over the same half-period, see Fig. 3. Therefore, the Chern-Simons number is always shifted in certain direction for some period of time *just before* the sphaleron transitions, making transitions with $\Delta N_{\text{CS}} = -\text{sign } \kappa$ more probable than transitions in opposite direction.

This description provides a simple estimate for net asymmetry created by baryogenesis after preheating. Assuming that every topological transitions effectively freezes the maximal positive or negative δN_{CS} that existed 1/4-period before, one obtains from Eq. (7) (here we also use Eqs. 2.1 and 2.2 of Ref. [4]):

$$\frac{dN_{\text{CS}}}{dt} = -\text{sign } \kappa \cdot (\delta N_{\text{CS}})_{\text{max}} \Gamma_{\text{sph}} = -\frac{\kappa g v L}{2\pi} \left(\frac{\sigma_{\text{max}}}{\sigma_c}\right)^2 \Gamma_{\text{sph}} \quad (9)$$

and from Eq. (8):

$$\frac{\Delta N_{\text{CS}}}{\kappa} \sim \partial_0\langle\phi^*\phi\rangle < 0. \quad (10)$$

(compare to Eq. (3)). Substituting into Eq. (9) parameter values from [3, 4], one obtains

$$\frac{dN_{\text{CS}}}{dt} \sim -0.3 \kappa \Gamma_{\text{sph}} \quad (11)$$

in reasonable agreement with numerical results, see Fig. 4.

Although baryogenesis after preheating is suppressed by inflaton-Higgs coupling g , it keeps going as long as topological transitions occur, see Eqs. (9) and (11), and isn't affected by the wash-out problem. It also shows how strongly the nontrivial dynamics can affect simple estimates in the style of Eq. (2).

3 Conclusions

Here we have shown that dynamical effects do play an important role in baryogenesis at/after preheating, what is typical for complicated nonequilibrium processes [7, 8]. A simple (1+1)-dimensional model of electroweak preheating-related baryogenesis, depending on initial parameter values, may subsequently pass through two dynamically distinct stages with different baryogenesis mechanisms producing baryonic asymmetry of opposite signs. The second stage that occurs after preheating is completely beyond the reach of straightforward diffusion approach commonly used for analysis of electroweak baryogenesis scenarios.

Acknowledgments

The author is deeply indebted to his collaborators: Juan García-Bellido, Alexander Kusenko and Mikhail Shaposhnikov. Presentation of these results at XXXV Rencontres de Moriond would be impossible without kind support of conference organizers. This work is supported in part by RBRF grant 98-02-17493a.

References

- [1] V.A. Kuzmin, V.A. Rubakov and M.E. Shaposhnikov, *Phys. Lett. B* **155**, 36 (1985).
- [2] For a review, see V.A. Rubakov and M.E. Shaposhnikov, *Usp. Fiz. Nauk* **166**, 493 (1996) [hep-ph/9603208]; A. Riotto and M. Trodden, *Ann. Rev. Nucl. Part. Sci.* **49**, 35 (1999) [hep-ph/9901362].
- [3] J. Garcia-Bellido, D. Grigoriev, A. Kusenko and M. Shaposhnikov, *Phys. Rev. D* **60**, 123504 (1999) [hep-ph/9902449].
- [4] J. Garcia-Bellido and D. Grigoriev, *JHEP* **0001**, 017 (2000) [hep-ph/9912515].
- [5] D. Grigoriev, M. Shaposhnikov and N. Turok, *Phys. Lett. B* **275**, 395 (1992).
- [6] D.Yu. Grigoriev, in: Procs. of the 10th Int. Seminar QUARKS-98 (<http://www.inr.ac.ru/~q98/proc/grigoriev.ps.gz>).
- [7] J. M. Cornwall and A. Kusenko, hep-ph/0001058.
- [8] B. Nauta, *Phys. Lett. B* **478**, 275 (2000) [hep-ph/0002164].

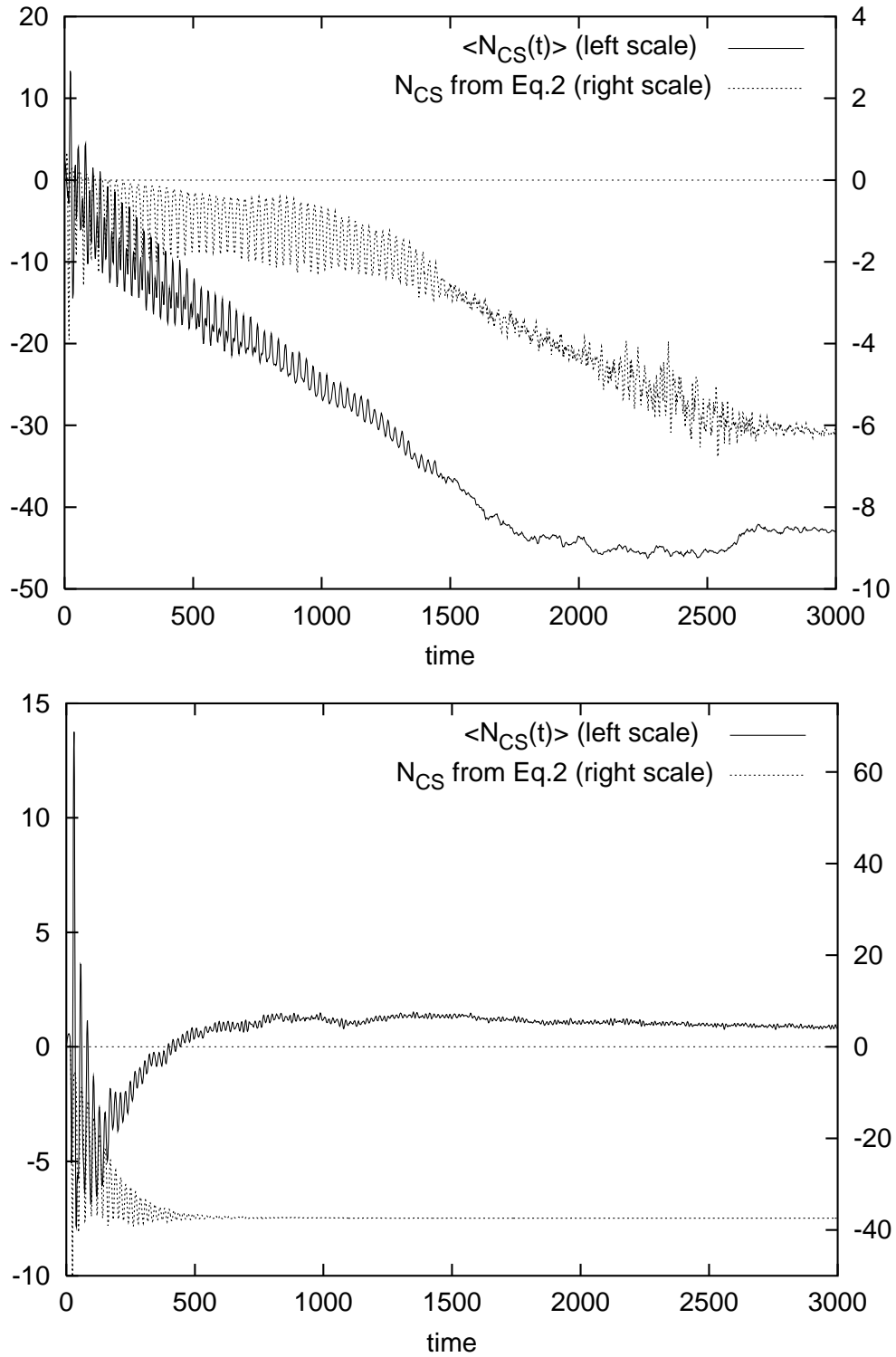


Figure 1: (upper plot) Time evolution of Chern-Simons number for $\kappa = -1$ and high $T_{rh} = 0.33 v$ (solid line, identical to Fig. 11 of Ref. [3]) compared to prediction of Eq. (2) (dotted line).

Figure 2: (lower plot) Same for reduced-energy runs of [3] with $\kappa = -1$ and $T_{rh} = 0.094 v$. On this plot $\langle N_{CS}(t) \rangle$, solid line, differs from Fig. 16 of Ref. [3] due to larger statistics. Strong discrepancy between observed $\langle N_{CS}(t) \rangle$ and that one predicted by diffusion equation (2) means that the baryogenesis at preheating, roughly described by Eq. (2), is followed here by some other baryoproduction mechanism — baryogenesis after preheating that moves N_{CS} in opposite direction.

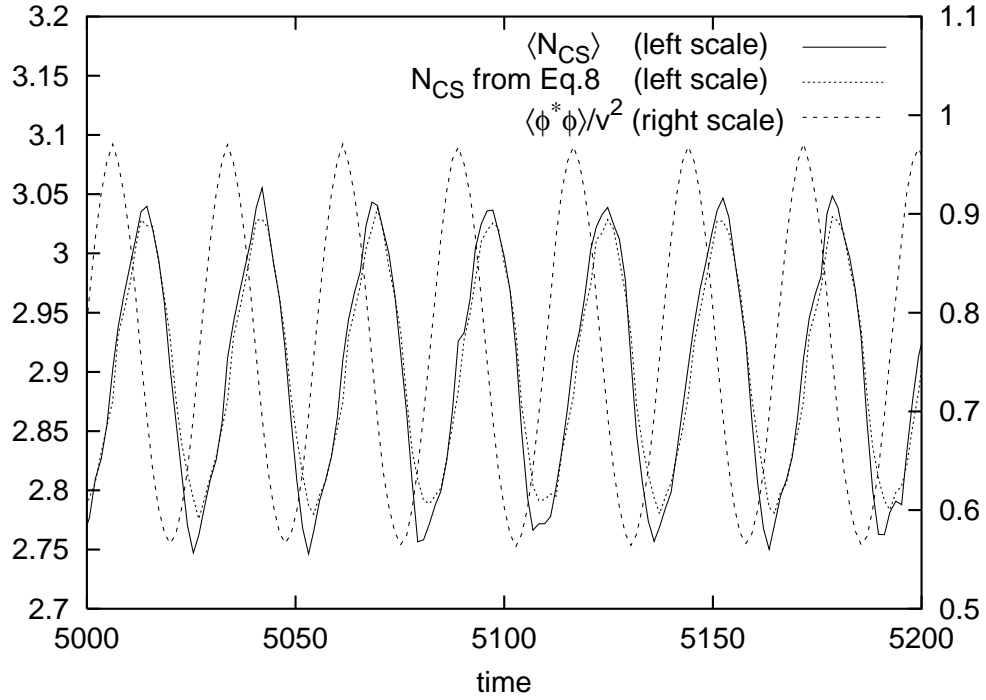
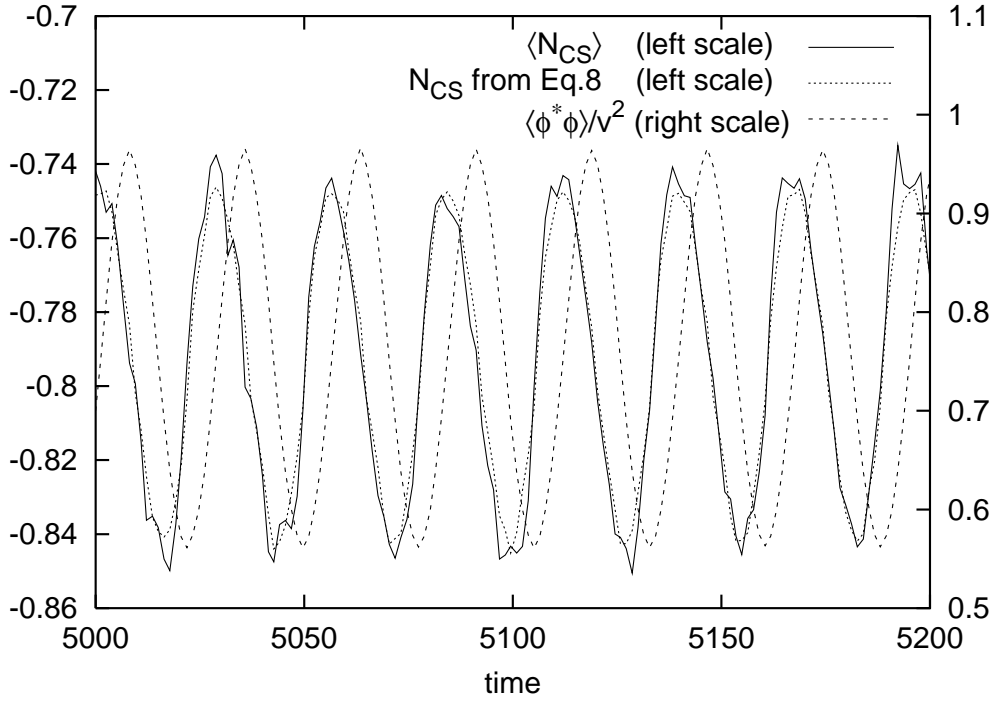


Figure 3: Comparison of phase relation between N_{CS} and $\langle\phi^*\phi\rangle$ oscillations for $\kappa = 0.1$ (upper plot) and $\kappa = -0.25$ (lower plot) shows that their relative phase shift is sensitive only to sign κ . Both plots also confirm Eq. (8). The sphaleron transitions occur when $\langle\phi^*\phi\rangle$ is at minimum and N_{CS} is close to its mean value N_0 , see text. Note that curves presented here are averaged over large ensemble of independent runs, so N_0 has non-integer values -0.8 and 2.9 , respectively.

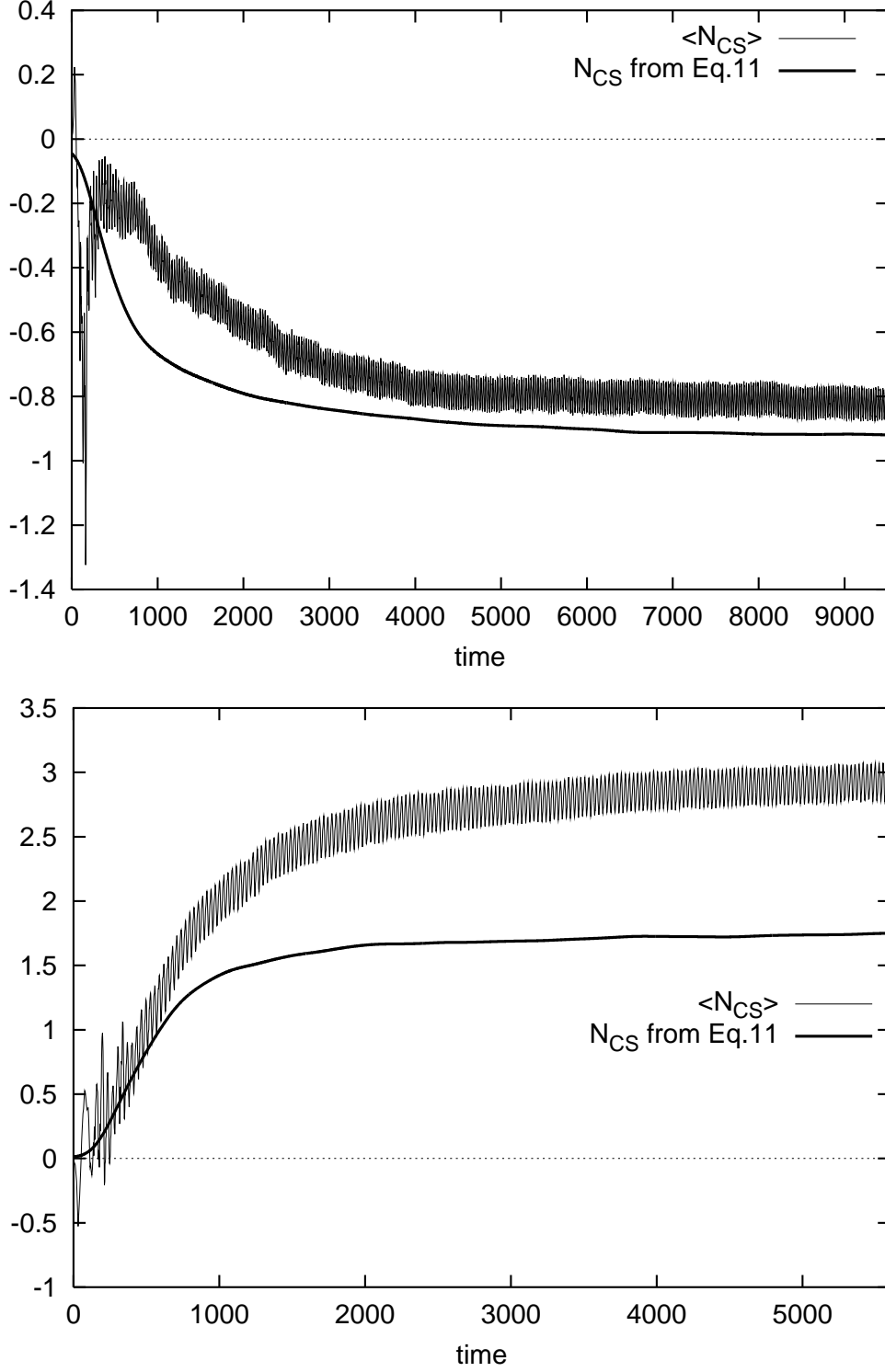


Figure 4: Eq. (11) adequately describes dynamics of Chern-Simons number both for $\kappa = 0.1$ (upper plot) and $\kappa = -0.25$ (lower plot), demonstrating the lack of wash-out for baryogenesis after preheating. Unlike Fig. 2, both $\langle N_{CS} \rangle$ curves can be smoothly interpolated to origin, due to the suppression of baryogenesis during preheating at very low $T_{rh} \sim 10^{-2}v$.